Conserv Genet
DOI 10.1007/s10592-009-9972-3

RESEARCH ARTICLE

Multilocus phylogenetic and coalescent analyses identify two cryptic species in the Italian bianchetto truffle, *Tuber borchii* Vittad.

Enrico Bonuso · Alessandra Zambonelli · Sarah E. Bergemann · Mirco Iotti · Matteo Garbelotto

Received: 12 January 2009 / Accepted: 5 August 2009

Abstract *Tuber borchii* (Ascomycota, Pezizales) is a highly valued truffle sold in local markets in Italy. Despite its economic importance, knowledge on its distribution and genetic structure is scarce. The objective of this work was to investigate the factors shaping the genetic structure of *T. borchii* using 61 representative specimens with a broad distribution throughout Italy. In spite of the lack of morphological differences, phylogenetic and coalescent-based analyses using four loci identified two genetically isolated groups sympatrically distributed. The low levels of divergence between the two clades may be the result of recent range expansions from geographically distinct refugia, potentially mediated by reforestation using coniferous species that are common ectomycorrhizal symbionts for both groups.

Keywords Cryptic species · Genetic isolation · Genetic subdivision

E. Bonuso · A. Zambonelli (✉) · M. Iotti
Dipartimento di Protezione e Valorizzazione Agroalimentare (DIPROVAL), University of Bologna, via Fanin 46, 40127 Bologna, Italy
e-mail: zambonel@agrsci.unibo.it

S. E. Bergemann
Biology Department, Middle Tennessee State University, PO Box 60, Murfreesboro, TN 37132, USA

M. Garbelotto
Department of Environmental Science, Policy, and Management, Ecosystem Sciences Division, University of California Berkeley, 137 Mulford Hall, Berkeley, CA 94720, USA

Introduction

Tuber borchii Vittad. (Ascomycota, order Pezizales, family Tuberaceae) is a widespread hypogeous fungus, forming commercially valued fruiting bodies in ectomycorrhizal symbiosis with a wide range of angiosperm and gymnosperm species (Hall et al. 2007). Because of its economic value, this species has recently been introduced into New Zealand (Hall 2007), and it is increasingly sought after in Italy, where it is known to be relatively abundant (Zambonelli et al. 2002). Furthermore, *T. borchii* is used as model for the study of fungus-plant molecular interactions (Lazzari et al. 2007) thanks to the development of a protocol for its mycorrhization in vitro with *Tilia platyphyllos* (Sisti et al. 1998).

In spite of its economical importance and scientific relevance, knowledge of geographical distribution and genetic variability of *T. borchii* is limited in comparison with other commercially valuable *Tuber* species (El Karkouri et al. 2007; Mello et al. 2005; Murat et al. 2004; Paolocci et al. 2004; Rubini et al. 2004, 2005; Wedén et al. 2004; Amicucci et al. 2000). Two contrasting patterns using nuclear ribosomal Internal Transcribed Spacers (ITS) marker have emerged for species within the genus *Tuber*. The first, exemplified by the works of Paolocci et al. (2004) and Wedén et al. (2005) on *T. aestivum*, is that of highly variable species both morphologically and genetically. The second, exemplified by the studies of Murat et al. (2004) and Mello et al. (2005) is that of limited variability detected within the prized truffles *T. melanosporum* and *T. magnatum*. Information on the phylogenetic relationships among truffle species is also currently available (Jeandroz et al. 2008) .

T. borchii belongs to the Puberulum clade or clade V among five ITS clades within the genus *Tuber* (Jeandroz

Published online: 22 August 2009

et al. 2008). This clade comprises most European, Asian and North American species of whitish truffles including *T. borchii*, *T. dryophilum* Tul., *T. foetidum* Vittad., *T. liui* A.S. Xu, *T. maculatum* Vittad., *T. oligospermum* (Tul. & C. Tul.) Trappe, *T. rapaeodorum* Tul., *T. scruposum* R. Hesse, *T. whetstonense* J.L. Frank, Southworth & Trappe, and three unidentified Chinese species (Jeandroz et al. 2008). As in other fungal groups, the significant morphological similarities among some species of whitish truffles within this clade, has led to frequent misidentifications. This taxonomic problem is exemplified by the conflicts between morphologically-based and sequence-based classifications, often resulting in the frequent misidentification of GenBank accessions (Hall et al. 2007; El Karkouri et al. 2007; Mello et al. 2006).

The increased demand for truffles and the decline of natural truffle production have resulted in the development of technologies for the cultivation and conservation of truffles (Hall et al. 2007). Despite these efforts, truffle production in Europe continues to decline as a result of deforestation, reforestation with unsuitable hosts, changes in forest management practices, global temperature changes, and increased acidification of soils (Hall et al. 2003, 2007). The assessment of genetic diversity in natural truffiéres represents an important conservation strategy to identify the spatial genetic diversity of *T. borchii* and to pinpoint source populations for in situ inoculations and the establishment of truffiéres in plantation settings. This study provides the first in-depth analysis of genetic diversity of *T. borchii* using multiple, nuclear loci to investigate genetic diversity and detailed studies of morphological characteristics of the ascomata between phylogenetical species of *T. borchii*.

Materials and methods

Source of samples

A total of 45 ascomata were collected in a 4-year period (2002–2006) in natural truffiéres. In addition, we obtained 16 pure cultures collected in northeastern Italy as described by Iotti et al. (2002) (Table 1). All samples were classified as *T. borchii* on the basis of their macroscopic and microscopic features and distinctive organoleptic properties (Pegler et al. 1993; Zambonelli et al. 2000b). Dry specimens were deposited in the herbarium of the "Centro di Micologia" of Bologna (CMI-UNIBO).

DNA extraction and PCR amplification

Genomic DNAs of the ascomata were isolated from 75 mg of lyophilized gleba (the spore-bearing tissue) or mycelium of each sample using DNeasy Plant Mini Kit (Qiagen, Hilden, Germany) according to the manufacturer's instructions. Extracts were eluted in 50 µl of sterile water and its DNA concentration was estimated using a spectrophotometer (Beckman Coulter Inc., Fullerton, CA, USA).

Four loci, including the nuclear ribosomal ITS, nuclear ribosomal Intergenic Spacers (IGS), protein kinase C (PKC) and beta-tubulin (β-tubulin) were Polymerase Chain Reaction (PCR) amplified from ascomata and cultures (Table 1). All PCR amplifications were performed using 25–50 ng of template DNA in a final volume of 25 µl containing 1× PCR buffer (Promega, Madison, WI, USA), 1.25 U of Taq DNA polymerase, 0.2 mM dNTPs and 0.4 µM each of forward and reverse primer. Cycling conditions and $MgCl_2$ concentrations varied depending on the target locus. ITS amplifications were performed using ITS1F and ITS4 (Gardes and Bruns 1993) following the protocol described by Amicucci et al. (1996). IGS PCR amplifications were performed using primers CNL12 and NS1r as described in Martin et al. (1999) from four ascomata and mycelia from four cultures (Tbo1/94, Tbo2352, Tbo2422, Tbo1570, Tbo2389, Tbo2445, Tb98 and Tbo2370). Alignments of the resulting sequences were generated using CLUSTAL W (Thompson et al. 2004) and used to design primers specific for the PCR amplification of the IGS region of *T. borchii*. We designed two primers, IGS-EB3 (5′-GGGTAACAATAGTGGTAGAGG-3′) and IGS-EB5 (5′-ACTTTTAATTGAGCATGAGGG-3′). PCR reactions were performed with 3 mM of $MgCl_2$, under the following conditions: 94°C for 3 min, 35 cycles of 94°C for 30 s, 30 s at 58°C, 72°C for 2 min 30 s and 10 min at 72°C. The β-tubulin region was PCR amplified with Bt2a and Bt2b (Glass and Donaldson 1995) after adjusting the $MgCl_2$ concentration to 2 mM. PKC regions were amplified with Pkc1f and Pkc1r (Wang et al. 2006) after adjusting $MgCl_2$ concentrations to 2.6 mM. PCR cycling conditions for β-tubulin and PKC were as follows: 95°C for 3 min, 30 cycles at 94°C for 30 s, 58°C (β-tubulin) or 59°C (PKC) for 45 s, and 72°C for 2 min followed by 72°C for 10 min.

Sequencing strategy and phylogenetic analyses

PCR products were purified using the Gene Clean II kit (BIO 101, Vista, CA, USA) and then bi-directionally sequenced. Sequence reactions were performed using the ABI PRISM 3700 DNA Analyzer (Applied Biosystems, Foster City, CA, USA) with Big Dye Terminator v3.1 chemistry according to the manufacturer instructions. After excluding the ambiguous regions at the 5′ and 3′ ends of the chromatograms, sequences were edited using Sequencher 4.6 (Gene Codes, Ann Arbor, MI, USA) and aligned

Table 1 Geographic location, source and GenBank accession numbers for samples of *Tuber borchii* collected from Italy

Sample	Source	Provenance (Province—Locality)	Accession number		Clade
1/94	Mycelium	Rovigo—Rosolina mare	ITS	FJ554472	I
			IGS	FJ598623	
			β-tubulin	FJ560915	
			PKC	FJ594253	
1570	Mycelium	Bologna—Sasso Marconi	ITS	FJ554466	I
			IGS	FJ598624	
			β-tubulin	FJ560917	
			PKC	FJ594251	
Tb98	Mycelium	Bologna—Guzzano	ITS	FJ554465	I
			IGS	FJ598625	
			β-tubulin	FJ560937	
			PKC	FJ594273	
2352	Mycelium	Rovigo—Porto Viro	ITS	FJ554470	I
			IGS	FJ598622	
			β-tubulin	FJ560920	
			PKC	FJ594255	
1999	Mycelium	Ravenna—Marina di Ravenna	ITS	FJ554467	I
			IGS		
			β-tubulin		
			PKC		
2292	Mycelium	Bologna—Pianoro	ITS	FJ554468	I
			IGS		
			β-tubulin		
			PKC		
2364	Mycelium	Rovigo—town cemetery	ITS	FJ554469	I
			IGS	FJ598635	
			β-tubulin	FJ560921	
			PKC	FJ594256	
2282	Mycelium	Bologna—Pianoro	ITS	FJ554471	I
			IGS	FJ598634	
			β-tubulin	FJ560919	
			PKC	FJ594254	
2/94	Mycelium	Rovigo—Rosolina mare	ITS	FJ554473	I
			IGS		
			β-tubulin		
			PKC		
1463	Mycelium	Ravenna—Marina di Ravenna	ITS	FJ554474	I
			IGS	FJ598632	
			β-tubulin	FJ560916	
			PKC	FJ594250	
10Ra	Mycelium	Ravenna—Marina di Ravenna	ITS	FJ554475	I
			IGS		
			β-tubulin		
			PKC		
2360	Ascoma	Ferrara—Lido delle Nazioni	ITS	FJ554477	I
			IGS		
			β-tubulin		
			PKC		

Table 1 continued

Sample	Source	Provenance (Province—Locality)	Accession number		Clade
2383	Ascoma	Bologna—Valpiana	ITS	FJ554480	I
			IGS		
			β-tubulin		
			PKC		
2387	Ascoma	Isernia—Belmonte del Sannio	ITS	FJ554481	I
			IGS		
			β-tubulin		
			PKC		
2359	Ascoma	Ferrara—Lido delle Nazioni	ITS	FJ554482	I
			IGS		
			β-tubulin		
			PKC		
2682	Ascoma	Palermo—San Martino delle Scale	ITS	FJ554484	I
			IGS	FJ598636	
			β-tubulin		
			PKC		
1833[a]	Ascoma	Reggio Emilia—Quattrocastella	ITS	FJ554485	I
			IGS	FJ598633	
			β-tubulin	FJ560918	
			PKC	FJ594252	
2389	Ascoma	Isernia—Belmonte del Sannio	ITS	FJ554483	I
			IGS	FJ598620	
			β-tubulin	FJ560923	
			PKC	FJ594258	
2445	Ascoma	Pavia—town park	ITS	FJ554490	I
			IGS	FJ598618	
			β-tubulin		
			PKC		
2370	Ascoma	Siena—town park	ITS	FJ554478	I
			IGS	FJ598621	
			β-tubulin	FJ560922	
			PKC	FJ594257	
2422	Ascoma	Modena—Santa Giulia	ITS	FJ554479	I
			IGS	FJ598619	
			β-tubulin	FJ560924	
			PKC	FJ594259	
2363[a]	Ascoma	Rovigo—town park	ITS	FJ554491	II
			IGS		
			β-tubulin		
			PKC		
3022	Ascoma	Ferrara—Bosco di Santa Giustina	ITS	FJ554492	II
			IGS	FJ598637	
			β-tubulin	FJ560939	
			PKC	FJ594260	
3026	Ascoma	Ferrara—Bosco Spada	ITS	FJ554493	II
			IGS	FJ598638	
			β-tubulin	FJ560925	
			PKC	FJ594261	

Table 1 continued

Sample	Source	Provenance (Province—Locality)	Accession number		Clade
3032	Ascoma	Ferrara—Bosco Spada	ITS	FJ554496	II
			IGS	FJ598626	
			β-tubulin	FJ560926	
			PKC	FJ594262	
3034[a]	Ascoma	Ferrara—Volano	ITS	FJ554497	II
			IGS	FJ598627	
			β-tubulin	FJ560927	
			PKC	FJ594263	
3042	Ascoma	Ferrara—Volano	ITS	FJ554487	I
			IGS	FJ598639	
			β-tubulin	FJ560928	
			PKC	FJ594264	
3052[a]	Mycelium	Ferrara—Volano	ITS	FJ554500	I
			IGS	FJ598628	
			β-tubulin	FJ560929	
			PKC	FJ594265	
3055	Ascoma	Ferrara—Volano	ITS	FJ554501	II
			IGS	FJ598629	
			β-tubulin	FJ560938	
			PKC	FJ594270	
3058	Ascoma	Ferrara—Gardelletta	ITS	FJ554506	I
			IGS	FJ598640	
			β-tubulin	FJ560941	
			PKC	FJ594275	
3064	Ascoma	Ferrara—Gran Bosco della Mesola	ITS	FJ554494	II
			IGS	FJ598642	
			β-tubulin	FJ560930	
			PKC	FJ594266	
3065	Ascoma	Ferrara—Gran Bosco della Mesola	ITS	FJ554502	II
			IGS	FJ598630	
			β-tubulin	FJ560931	
			PKC	FJ594271	
3067[a]	Mycelium	Ferrara—Dosso	ITS	FJ554503	II
			IGS		
			β-tubulin	FJ560932	
			PKC	FJ594267	
3078[a]	Ascoma	Palermo—San Martino delle Scale	ITS	FJ554495	II
			IGS		
			β-tubulin		
			PKC		
3087	Ascoma	Ferrara—Vascello d'Oro	ITS	FJ554507	I
			IGS	FJ598643	
			β-tubulin	FJ560942	
			PKC	FJ594276	
3088	Ascoma	Ferrara—Lido di Spina	ITS	FJ554489	I
			IGS		
			β-tubulin		
			PKC		

Table 1 continued

Sample	Source	Provenance (Province—Locality)	Accession number		Clade
3091	Ascoma	Ferrara—Lido di Spina	ITS	FJ554488	I
			IGS	FJ598644	
			β-tubulin	FJ560933	
			PKC		
3113	Ascoma	Ferrara—Romanina	ITS	FJ554498	II
			IGS		
			β-tubulin		
			PKC		
3116	Ascoma	Ferrara—Goara	ITS	FJ554499	II
			IGS	FJ598645	
			β-tubulin	FJ560934	
			PKC	FJ594272	
3120	Ascoma	Ferrara—Goara	ITS	FJ554504	II
			IGS	FJ598631	
			β-tubulin	FJ560935	
			PKC	FJ594268	
17Bo	Mycelium	Ravenna—Marina di Ravenna	ITS	DQ679802	I
			IGS		
			β-tubulin	FJ560940	
			PKC	FJ594274	
1Bo	Mycelium	Ravenna—Marina di Ravenna	ITS	FJ554476	I
			IGS		
			β-tubulin		
			PKC		
43Bo	Mycelium	Ravenna—Marina di Ravenna	ITS	FJ554505	I
			IGS	FJ598646	
			β-tubulin	FJ560936	
			PKC	FJ594269	
3060	Ascoma	Ferrara—Gardelletta	ITS	FJ554486	I
			IGS	FJ598641	
			β-tubulin		
			PKC		
3262[a]	Ascoma	Rovigo—Rosolina mare	ITS	FJ554508	I
			IGS		
			β-tubulin		
			PKC		
3263[a]	Ascoma	Ferrara—Gardelletta	ITS	FJ554509	I
			IGS		
			β-tubulin		
			PKC		
3264[a]	Ascoma	Ferrara—Volano	ITS	FJ554510	I
			IGS		
			β-tubulin		
			PKC		
3294[a]	Ascoma	Bari—town park	ITS	FJ554511	I
			IGS		
			β-tubulin		
			PKC		

Table 1 continued

Sample	Source	Provenance (Province—Locality)	Accession number		Clade
3299[a]	Ascoma	Palermo—Monte Petroso	ITS	FJ554512	I
			IGS		
			β-tubulin		
			PKC		
3300	Ascoma	Palermo—Monte Petroso	ITS	FJ554513	I
			IGS		
			β-tubulin		
			PKC		
3404	Ascoma	Ferrara—Bosco Spada	ITS	FJ554517	II
			IGS		
			β-tubulin		
			PKC		
3257	Ascoma	Ferrara—Bosco Spada	ITS	FJ554518	II
			IGS		
			β-tubulin		
			PKC		
3260[a]	Ascoma	Ferrara—Gran Bosco della Mesola	ITS	FJ554519	II
			IGS		
			β-tubulin		
			PKC		
3402[a]	Ascoma	Ferrara—Gran Bosco della Mesola	ITS	FJ554520	II
			IGS		
			β-tubulin		
			PKC		
3405[a]	Ascoma	Ferrara—Bosco di Santa Giustina	ITS	FJ554521	II
			IGS		
			β-tubulin		
			PKC		
3256[a]	Ascoma	Ferrara—Bosco di Santa Giustina	ITS	FJ554522	II
			IGS		
			β-tubulin		
			PKC		
3258[a]	Ascoma	Ferrara—Bosco di Santa Giustina	ITS	FJ554514	I
			IGS		
			β-tubulin		
			PKC		
3259[a]	Ascoma	Ferrara—Bosco di Santa Giustina	ITS	FJ554515	I
			IGS		
			β-tubulin		
			PKC		
3401[a]	Ascoma	Ferrara—Bosco di Santa Giustina	ITS	FJ554523	II
			IGS		
			β-tubulin		
			PKC		
3403[a]	Ascoma	Ferrara—Bosco di Santa Giustina	ITS	FJ554524	II
			IGS		
			β-tubulin		
			PKC		

Table 1 continued

Sample	Source	Provenance (Province—Locality)	Accession number		Clade
3298[a]	Ascoma	Palermo—Monte Petroso	ITS	FJ554516	I
			IGS		
			β-tubulin		
			PKC		

[a] Isolates included in morphological analyses

by CLUSTAL W (Thompson et al. 2004) using default settings and manually optimized with Bioedit version 5.0.9 (Hall 1999).

We performed phylogenetic analyses of four nuclear loci (ITS, IGS, β-tubulin and PKC) using maximum likelihood (ML) and maximum parsimony (MP) for each single locus, and Bayesian estimation (BI) with concatenation of the four loci into a single alignment. ML and MP analyses were implemented in PAUP 4.0b10 (Swofford 2000) with gaps treated as missing data. MP trees were found by using the tree bisection reconnection (TBR) branch swapping algorithm, with randomized stepwise addition of taxa under the heuristic search method. When more than one MP tree was found, the 50% major-rule consensus tree was calculated from all MP trees. For both ML and MP internal branch support was assessed by bootstrap (BS) analysis of 1,000 replicates with 10 random additions per replicate using FastStep algorithm (Felsenstein 1985).

To determine the best-fit model of DNA evolution (Posada and Crandall 1998) and reduce the systematic errors inherent to unpartioned models of multiple concatenated alignment (Brandley et al. 2005; Castoe and Parkinson 2006), Modeltest v 3.06 was run for each locus using the Akaike information criterion (AIC) to assess model fit on 56 different models (Posada and Buckley 2004). Bayesian posterior probabilities were calculated using MrBAYES 3.1.2 (Huelsenbeck and Ronquist 2001) specifying a general time-reversible model with variable rates, one run of 1,000,000 generations sampling every 1,000 generations was performed with four cold and three heated Markov Chain Monte Carlo (MCMC) chains. After excluding samples taken prior to stationarity, posterior probability distributions were used to compute a 50% majority rule consensus tree.

Population subdivision and gene flow

To test for population subdivision and gene flow, we used ML or Bayesian estimation approaches in SNAP (Suite of Nucleotide Analysis Programs) Workbench (Price and Carbone 2005). ITS, IGS, β-tubulin and PKC alignments were analyzed after the concatenation into a single alignment using SNAP Combine (Aylor et al. 2006) and their sequences were collapsed into unique haplotypes after excluding INDELs (SNAP Map; Aylor et al. 2006). Site incompatibilities matrices were generated in SNAP Clade and visualized using SNAP Matrix (Markwordt et al. 2003). Permtest was used to calculate Hudson's test for population subdivision by implementing a MCMC procedure (Hudson et al. 1992). In subdivided populations, MDIV (Nielsen and Wakeley 2001) was used to estimate θ ($\theta = 2Nefu$, where Nef is the female-effective population size and u is the per locus mutation rate), migration rate ($M = 2Nefm$, where m is the migration rate), time of population divergence ($T = t/Nef$, where t is generation time) and time to most recent common ancestor ($TMRCA = tu$). We recognize that estimates of θ, T, M, and TMRCA may be problematic given that this model does not jointly estimate parameters for both subpopulations as performed in IM (Hey and Nielsen 2004); however, we have used this program only to differentiate between recurrent gene flow from shared ancestral polymorphisms among samples from two different clades. We used a maximum-likelihood (ML) approach implemented in MIGRATE 2.0.6 (Beerli and Felsenstein 1999) to infer asymmetric patterns of gene flow between the two populations. We calculated migration (m), on the basis of the neutral parameter theta (θ), which is equivalent to $4Neu$ ($4 \times$ the effective population size $Ne \times$ the mutation rate) for nuclear loci. These tests were performed using an infinite sites model, 10 short shorts, sampling 50,000 genealogies and with a sampling increment of 20 genealogies, followed by five long chains, each with a total of 100,000 genealogies and a sampling increment of 20 genealogies. The first 10,000 genealogies in each chain were discarded (Beerli and Felsenstein 2001). Ten independent runs were computed with 10 random starting seeds in order to establish whether migration (m) estimates converged.

Morphological studies

Morphological characterization was carried out on sections of 10 ascomata from each of the two clades identified by phlyogenetic analyses. After ascomata were fixed in FAA (formaldehyde:acetic acid:70% ethanol, 5:5:90), we

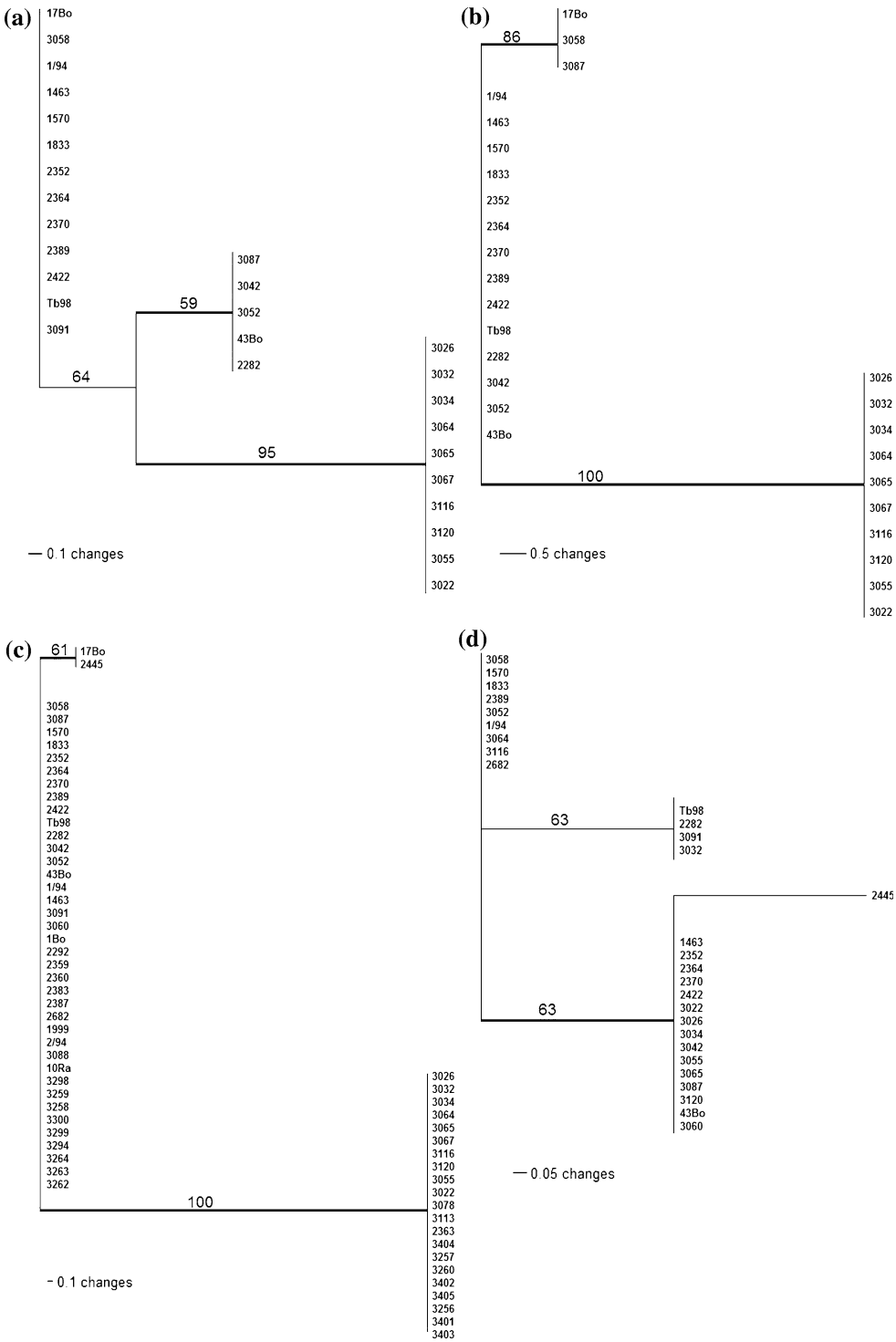

Fig. 1 MP phylogram trees produced from alignment of four nuclear DNA loci sequenced from Italian *Tuber borchii*: **a** beta-tubulin (β-tubulin); **b** protein kinase C (PKC); **c** nuclear ribosomal Internal Transcribed Spacers (ITS); **d** nuclear ribosomal Intergenic Spacers (IGS). *Thickened branches* indicate those that are supported both by parsimony bootstrap values of >70% and by Bayesian posterior probabilities of >95%

estimated the thickness of peridium, dimensions of external peridium cells (area, perimeter, equivalent diameter, maximum and minimum Feret's diameter) (Walton 1948); size of cystidia (length and basal diameter); dimensions of spores from asci containing three spores (area, perimeter, equivalent diameter, maximum and minimum Feret's diameter); spore ornamentation length; spore mesh width (area, perimeter, equivalent diameter, maximum and minimum Feret's diameter). Sections from each analyzed ascoma (8–10 μm thick) were obtained manually or with a rotary cryomicrotome (Tissue Tek II, Naperville, IL, USA) embedding in Tissue Tek OCT compound. Serial sections were mounted in lactic acid and observed under a Nikon ECLIPSE TE 2000-E microscope (Nikon, Melville, NY, USA) at 400× and 1,000× magnification. Measures were recorded using NIS-Elements AR 2.20 software

(Laboratory Imaging, Prague, Czech Republic) from images captured with a Nikon DXM1200F digital camera.

In order to quantify the differences in shape of external peridium cells and of spores, we adopted the index of lobation as an index of roundness by estimating the perimeter and the area (Giomaro et al. 2000). Mean values of morphological parameter for each specimen were calculated and statistical analyses were performed using the nonparametric Mann–Whitney *U* Test by testing the significance at $\alpha = 0.05$ level after Bonferroni correction for multiple pairwise comparisons. To determine whether morphological characteristics of peridium and spores are able differentiate between samples from each phylogenetic species, we applied discriminant analysis. All statistical analyses were performed using R 2.9 software (R Development Core Team 2006).

Results

Phylogenetic analyses

The IGS locus was PCR amplified from 29 samples, the ITS from 61, the β-tubulin from 28, and the PKC region from 27 samples. We generated an alignment of 564 nucleotides (nt) with 11 parsimony informative and 1 parsimony uninformative characters for the ITS locus (8 and 4 in the ITS1 and ITS2 regions, respectively), an IGS alignment with 865 nt and 2 parsimony informative characters, 1 uninformative and one excluded insertion found in a single isolate (isolate 1463, Table 1), an alignment of 441 nt with 5 parsimony informative characters for the β-tubulin region and an alignment of 1,091 nt with 12 parsimony informative characters for the PKC region. In total the combined ITS, β-tubulin, PKC, and IGS data set was composed of 2,961 characters; from these 2,961 characters, 2,929 (99%) were constant, 30 (1%) were parsimony informative and 2 characters were parsimony uninformative.

Sequences of the four loci were analyzed phylogenetically both separately and as a combined dataset. MP and ML analyses gave congruent topology for each of the four loci, thus only MP phylograms are shown (Fig. 1). Statistics of the trees obtained from each locus are reported in Table 2. Although the sets of isolates used for the four loci were not identical, results from β-tubulin, PKC and ITS all showed the presence of two well-supported clades without any correlation to geographical provenance (Fig. 3). Analyses based on these three loci resulted in concordant topologies with a clear partitioning in the same two clades. The IGS dataset was not concordant with the three other loci (ITS, β-tubulin, PKC) or with the combined dataset, giving a tree topology with four different clades. Despite this discrepancy, the consensus phylogram built with the 50% majority-rule using the combined dataset with the four loci confirmed the presence of two well supported clades (Fig. 2).

Population subdivision and gene flow

Based on Hudson's test (Kst: 0.270833, Ks: 8.40, Kt: 11.520, $P = 0.007$) the two clades identified in this study are genetically isolated. When testing for current gene flow using MDIV, the posterior distribution included zero an indication of lack of recurrent gene flow among individuals belonging to the two clades. MIGRATE was used instead to estimate the direction and extent of migration over the history of the sample. We found evidence to support asymmetric migration from Clade 1 to Clade 2 ($m = 864$–1,364), but no migration from Clade 2 to Clade 1 ($m = 0$). The absence of ongoing inter-specific gene flow coupled with asymmetric gene flow, suggests that the two populations currently represent two distinct gene pools, a pattern consistent with genetic isolation and speciation.

Morphological studies

Macroscopic and microscopic features of all ascomata independent of clade of origin were consistent with morphological characters of *T. borchii* (Vittadini 1831; Pegler

Table 2 Statistic of the trees obtained with single loci and concatenated data set of three concordant loci (ITS + β-tubulin + PKC) and four loci (ITS-5.8S + β-tubulin + PKC + IGS) of *Tuber borchii*

	Tree length	CI	CIx	RI	RC	HI	HIx
ITS-5.8S	12	1.00	1.00	1.00	1.00	0.00	0.00
β-tubulin	5	1.00	–	1.00	1.00	0.00	–
PKC	12	1.00	–	1.00	1.00	0.00	–
IGS	3	1.00	1.00	1.00	1.00	0.00	0.00
ITS-5.8S + β-tubulin + PKC	38	0.763	0.757	0.962	0.734	0.237	0.243
ITS-5.8S + β-tubulin + PKC + IGS	53	0.566	–	0.896	0.507	0.434	–

CI consistency index, *CIx* consistency index excluding uninformative characters, *RI* retention index, *RC* rescaled consistency index, *HI* homoplasy index, *HIx* homoplasy index excluding uninformative characters

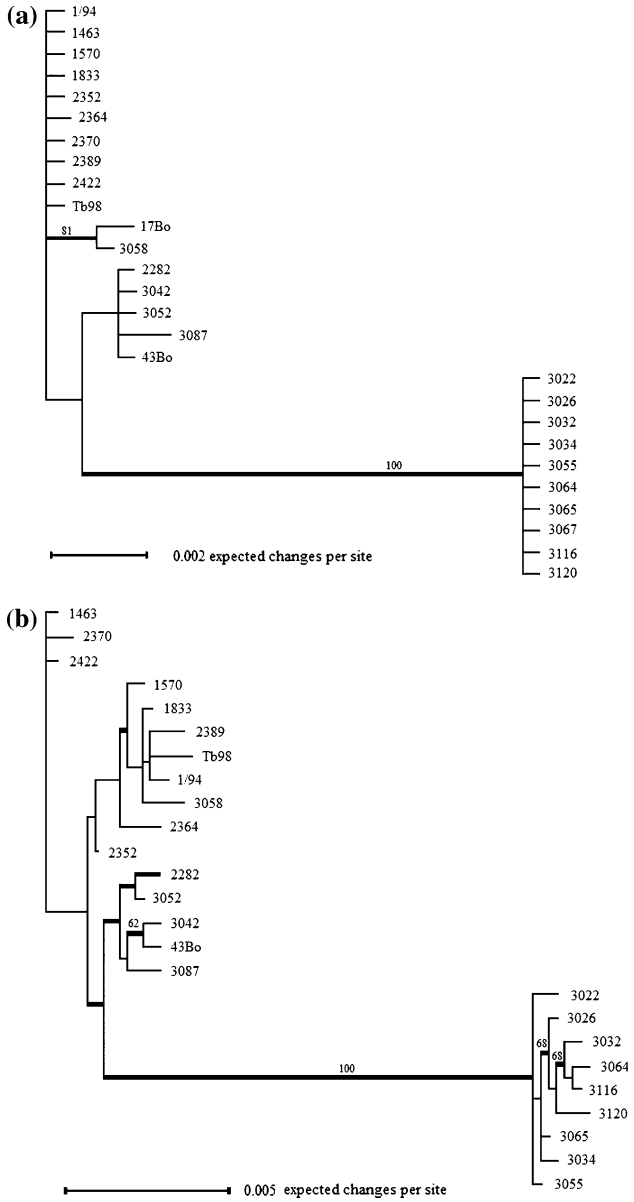

Fig. 2 MP phylogram trees resulting from combined analysis of three concordant nuclear DNA loci (β-tubulin; protein kinase C and Internal Transcribed Spacers) (**a**) and four nuclear loci (β-tubulin; protein kinase C; Internal Transcribed Spacers; Intergenic Spacer) (**b**) of *Tuber borchii*. Thickened branches indicate those that are supported both by parsimony bootstrap values of > 70% and by Bayesian posterior probabilities of >95%

et al. 1993; Ceruti et al. 2003; Zambonelli et al. 2000b). The Mann–Whitney Test *U* showed no significant differences between the morphological characters of isolates grouped into two clades (Table 3). These results were confirmed in the discriminant analysis by the low level of separation between individuals belonging to the two clades. Morphological characterization of the peridium and spores could result in correct classification for 47% and 70% of the ascomata respectively.

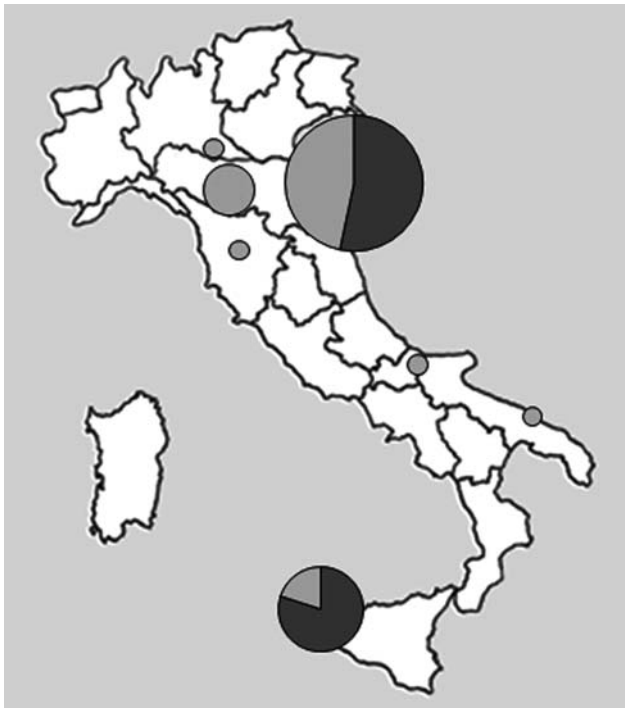

Fig. 3 Geographical distribution of the two phylogenetic species identified *in Tuber borchii* (clade 1 in *pale grey*, clade 2 in *dark grey*)

Discussion

We set out to determine the levels of genetic diversity and investigate the overall genetic structure of the Italian white truffle *T. borchii*. Combined and individually, the four loci analyzed showed a very low level of genetic diversity within the sampled ascomata but at the same time confirmed the phylogenetic separation of isolates into two clades. In spite of the incongruent results between the IGS and the other three loci, overall results indicated the presence of two clades that show no evidence of ongoing interspecific gene flow. Phylogenetic analyses based on the IGS locus produced a phylogeny with a tree topology that was not concordant with the topology obtained either by analysis of the other three loci individually, or by the combined analysis of all four loci. Since only two parsimony informative characters were present in the IGS, we hypothesize that the lack of congruence between the IGS and the other nuclear loci is likely the result of incomplete lineage sorting. Although a phylogenetic analysis inclusive of an appropriate taxon as an outgroup could have helped to discern the ancestral lineage between the two discovered in this study, our goal was mainly to infer the presence or absence of genetic and morphological sub-structuring within *T. borchii.*

Global temperature fluctuations during the Pleistocene (10,000–1,800,000 ybp) are known to have altered habitat ranges for numerous taxa creating complex patterns of

Table 3 The mean values of morphological measurements of peridium, cystidia and spores of two phylogenetic species of *Tuber borchii*

Morphological characters	Clade 1 Mean (SE)	Clade 2 Mean (SE)
Thickness of peridium (μm)	265 (22)	308 (21)
External peridium cells		
Area (μm^2)	83 (11)	59 (6)
Perimeter (μm)	34 (2)	29 (2)
Equivalent diameter (μm)	9.8 (0.6)	8.4 (0.4)
Maximum Feret diameter (μm)	12.5 (0.8)	11.0 (0.6)
Minimum Feret diameter (μm)	8.3 (0.5)	7.0 (0.3)
Index of roundness	1.08	1.11
Peridium cystidia		
Lenght (μm)	55.2 (5.0)	49.6 (3.5)
Basal diameter (μm)	4.3 (0.2)	4.3 (0.2)
Spores		
Area (μm^2)	610 (35)	631 (15)
Perimeter (μm)	87 (2)	89 (0.9)
Equivalent diameter (μm)	27.5 (0.8)	28.0 (0.3)
Maximum Feret diameter (μm)	30.0 (0.8)	30.3 (0.3)
Minimum Feret diameter (μm)	25.5 (0.7)	26.1 (0.3)
Index of roundness	1.01	1.01
Spore ornamentation length (μm)	4.0 (0.2)	4.4 (0.2)
Spore mesh width		
Area (μm^2)	29 (2)	34 (2)
Perimeter (μm)	20 (1)	22 (1)
Equivalent diameter (μm)	6.0 (0.2)	6.5 (0.2)
Maximum Feret diameter (μm)	7.1 (0.2)	7.7 (0.2)
Minimum Feret diameter (μm)	5.6 (0.1)	6.0 (0.2)

Means were obtained from 10 different ascomata. *SE* standard error

genetic diversity as a result of range contractions followed by post glacial expansions (Hewitt 1996, 2000). We propose that climatic fluctuations during the Pleistocene era may have lead to the spatial segregation resulting in genetic divergence among populations occupying different refugia, a scenario similar to that observed in *Tuber melanosporum* (Murat et al. 2004). The current sympatric geographic distribution of the two phylogenetic distinct taxa could be the result of a recent range expansion, following isolation in refugia, as reported for other taxa occupying similar geographic ranges (Hewitt 1996, 2000). In addition, the current sympatry of the two clades may in part be explained by human-mediated movements. *Tuber borchii* can colonize pine seedlings (Zambonelli et al. 2000a) as well as mature broadleaf and conifer species (Zambonelli et al. 2002), a pattern inconsistent with the habitat separation and partitioning across hosts as reported for other valuable *Tuber* species (Mello et al. 2005; Murat et al. 2004; Rubini et al. 2005; Wedén et al. 2004). Since most of the samples were taken were collected in pine plantations or reforested areas no longer used for timber production, it is possible that reforestation activities may have lead to the introduction of *T. borchii* and thus, has generated an overlap between the ranges of two phylogenetic species that occupied geographically disparate populations.

We were unable to identify any distinctive morphological features between the two genetically isolated groups, among several microscopic characters analyzed for ten ascomata from each clade. The presence of genetically isolated lineages among samples morphologically indistinguishable and traditionally described as *T. borchii* is one further example highlighting the complexity of species definition and taxa delimitations in the Fungi (Taylor et al. 2000, 2006). We support the notion that phylogenetic separation is the result of genetic isolation and that these genetically isolated lineages may represent two phylogenetic or cryptic species that have yet to undergo morphological differentiation.

The inconsistency between morphology of the ascomata and phylogenetic characters further complicates the classification of *T. borchii*, since traditional species classification relies heavily on both aspects. The commercial value of *T. borchii* is determined by macroscopic features of the ascomata and commercialization is driven by their organoleptic features (e.g. taste and aroma) of the ascomata. The taxonomical identification of *T. borchii* into two phylogenetic taxa having similar features should be taken in consideration when molecular identification of commercial truffle or of inoculated plants for truffle cultivation is carried out. Nonetheless, both lineages should be included in the commercially sought-after *T. borchii* maybe using a *sensu lato* definition; in the case of *Tricholoma matsutake* and *Boletus edulis*, for instance, several phylogenetic species are consistently sold at market (Chapela and Garbelotto 2004; Hall et al. 1998).

In summary, this study provides evidence to support the presence of two phylogenetically divergent gene pools (cryptic species) with no recurrent inter-specific gene flow within a commercially valuable species of truffles, and the presence of low genetic diversity within each phylogenetic species. Cumulatively, our data indicate the current distribution of these two phylogenetic species with overlapping geographic ranges possibly as a result of human activities. Future studies need to determine the possible presence of subtle phenotypic or ecological differences between these two cryptic species, and to further study the impact of human-mediated movement on the distribution of this commercially valuable ectomycorrhizal fungus. This information is not only of scientific interest, but it is also needed to design policies aimed at the conservation and enhancement of diverse assemblages of economic and

ecologically important symbiotic fungi. In *T. borchii*, we have identified two divergent lineages that at present are important sources of genetic diversity and sources of inoculum for the production of artificial truffiéres in plantation settings.

Acknowledgments We would like to thank Dr. Enrico Lancellotti for his assistance in statistical analyses of morphological data.

References

Amicucci A, Rossi I, Potenza L, Zambonelli A, Agostini D, Palma F, Stocchi V (1996) Identification of ectomycorrhizae from *Tuber* species by RFLP analysis of the ITS region. Biotechnol Lett 18:821–826. doi:10.1007/BF00127896

Amicucci A, Guidi C, Zambonelli A, Potenza L, Stocchi V (2000) Multiplex PCR for the identification of white *Tuber* species. FEMS Microbiol Lett 189:265–269. doi:10.1111/j.1574-6968.2000.tb09241.x

Aylor DL, Price EW, Carbone I (2006) SNAP: combine and map modules for multilocus population genetic analysis. Bioinformatics 22:1399–1401. doi:10.1093/bioinformatics/btl136

Beerli P, Felsenstein J (1999) Maximum likelihood estimation of migration rates and effective population numbers in two populations. Genetics 152:763–773

Beerli P, Felsenstein J (2001) Maximum likelihood estimation of a migration matrix and effective population sizes in *n* subpopulations by using a coalescent approach. PNAS 98:4563–4568. doi:10.1073/pnas.081068098

Brandley MC, Schmitz A, Reeder T (2005) Partitioned Bayesian analyses, partition choice and phylogenetic relationships of scincid lizards. Syst Biol 54:373–390. doi:10.1080/10635150590946808

Castoe TA, Parkinson CL (2006) Bayesian mixed models and the phylogeny of pitvipers (Serpentes: Viperidae). Mol Phylogenet Evol 39:91–110. doi:10.1016/j.ympev.2005.12.014

Ceruti A, Fontana A, Nosenzo C (2003) Le Specie Europee del Genere *Tuber*. Museo Regionale di Scienze Naturali, Torino

Chapela IH, Garbelotto M (2004) Phylogeography and evolution in Matsutake and close allies inferred by analyses of ITS sequences and AFLPs. Mycologia 96:730–741

El Karkouri K, Murat C, Zampieri E, Bonfante P (2007) Identification of internal transcribed spacer sequence motifs in truffles: a first step toward their DNA bar coding. Appl Environ Microb 73(16):5320–5330. doi:10.1128/AEM.00530-07

Felsenstein J (1985) Confidence limits on phylogenies: an approach using the bootstrap. Evolution 39:783–791

Gardes M, Bruns TD (1993) ITS primers with enhanced specificity for basidiomycetes—application to the identification of mycorrhizae and rusts. Mol Ecol 2:113–118

Giomaro G, Zambonelli A, Sisti D, Cecchini M, Evangelista V, Stocchi V (2000) Anatomical and morphological characterization of mycorrhizas of five strains of *Tuber borchii* Vittad. Mycorrhiza 10:107–114. doi:10.1007/s005720000065

Glass LN, Donaldson GC (1995) Development of primer sets designed for use with the PCR to amplify conserved genes from filamentous Ascomycetes. Appl Environ Microb 61:1323–1330

Hall TA (1999) BioEdit: a user-friendly biological sequence alignment editor and analysis program for Windows 95/98/NT. Nucleic Acids Symp Ser 41:95–98

Hall IR (2007) Truficultura en Nueva Zelanda. In: Reynas DS (ed) Truficultura. Fundamentos y técnicas Ediciones Mundi-Prensa, Madrid, pp 495–502

Hall IR, Lyon AJE, Wang Y, Sinclair L (1998) Ectomycorrhizal fungi with edible fruiting bodies. 2. *Boletus edulis*. Econ Bot 52:44–56. doi:10.1007/BF02861294

Hall IR, Wang Y, Amicucci A (2003) Cultivation of edible ectomycorrhizal mushrooms. Trends Biotechnol 21:433–438. doi:10.1016/S0167-7799(03)00204-X

Hall IR, Brown G, Zambonelli A (2007) Taming the truffle. The history lore and science of the ultimate mushroom. Timber, Portland

Hewitt GM (1996) Some genetic consequences of ice age, and their role in divergence and speciation. Biol J Linn Soc 58:247–276

Hewitt G (2000) The genetic legacy of the quaternary ice ages. Nature 405:907–913

Hey J, Nielsen R (2004) Multilocus methods for estimating population sizes, migration rates and divergence time, with applications to the divergence of *Drosophila pseudoobscura* and *D. persimilis*. Genetics 167:747–760

Hudson RR, Slatkin M, Maddison WP (1992) Estimation of levels of gene flow from DNA sequence data. Genetics 132:583–589

Huelsenbeck JP, Ronquist F (2001) MRBAYES: Bayesian inference of phylogenetic trees. Bioinformatics 17:754–755

Iotti M, Amicucci A, Stocchi V, Zambonelli A (2002) Morphological and molecular characterisation of mycelia of some *Tuber* species in pure culture. New Phytol 155:499–505. doi:10.1046/j.1469-8137.2002.00486.x

Jeandroz S, Murat C, Wang Y, Bonfante P, Le Tacon F (2008) Molecular phylogeny and historical biogeography of the genus *Tuber*, the 'true truffles'. J Biogeogr 35(5):815–829. doi:10.1111/j.1365-2699.2007.01851.x

Lazzari B, Caprera A, Cosentino C, Stella A, Milanesi L, Viotti A (2007) ESTuber db: an online database for *Tuber borchii* EST sequences. BMC Bioinformatics 8(Suppl 1):S13. doi:10.1186/1471-2105-8-S1-S13

Markwordt J, Doshi R, Carbone I (2003) Snap clade and matrix. Department of Plant Pathology, North Carolina State University, Raleigh. Available via DIALOG. http://www.cals.ncsu.edu/plantpath/faculty/carbone/home.html Accessed 15 Jan 2008

Martin F, Selosse MA, Tacon FL (1999) The nuclear rDNA intergenic spacer of the ectomycorrhizal basidiomycete *Laccaria bicolor*: structural analysis and allelic polymorphism. Microbiology 145:1605–1611

Mello A, Murat C, Vizzini A, Gavazza V, Bonfante P (2005) *Tuber magnatum* Pico, a species of limited geographical distribution: its genetic diversity inside and outside a truffle ground. Environ Microbiol 7:55–65. doi:10.1111/j.1462-2920.2004.00678.x

Mello A, Murat C, Bonfante P (2006) Truffles: much more than a prized and local fungal delicacy. FEMS Microbiol Lett 260(1):1–8. doi:10.1111/j.1574-6968.2006.00252.x

Murat C, Díez J, Luis P, Delaruelle C, Dupré C, Chevalier G, Bonfante P, Martin F (2004) Polymorphism at the ribosomal DNA ITS and its relation to postglacial re-colonization routes of the Perigord truffle *Tuber melanosporum*. New Phytol 164:401–441. doi:10.1111/j.1469-8137.2004.01189.x

Nielsen R, Wakeley J (2001) Distinguishing migration from isolation: a Markov chain Monte Carlo approach. Genetics 158:885–896

Paolocci F, Rubini A, Riccioni C, Topini F, Arcioni S (2004) *Tuber aestivum* and *Tuber uncinatum*: two morphotypes or two species? FEMS Microbiol Lett 235:109–115. doi:10.1016/j.femsle.2004.04.029

Pegler DN, Spooner BM, Young TWK (1993) British truffles. A revision of British hypogeous fungi. Royal Botanic Garden, Kew

Posada D, Buckley TR (2004) Model selection and model averaging in phylogenetics: advantages of Akaike information criterion and Bayesian approaches over likelihood ratio tests. Syst Biol 53:793–808. doi:10.1080/10635150490522304

Posada D, Crandall KA (1998) Modeltest: testing the model of DNA substitution. Bioinformatics 14:817–818

Price EW, Carbone I (2005) SNAP: workbench management tool for the evolutionary population genetic analysis. Bioinformatics 21:402–404. doi:10.1093/bioinformatics/bti003

R Development Core Team (2006) R: a language and environment for statistical computing. http://www.Royal-project.org

Rubini A, Topini F, Riccioni C, Paolocci F, Arcioni S (2004) Isolation and characterization of polymorphic microsatellite loci in white truffle (*Tuber magnatum*). Mol Ecol Notes 4:116–118. doi:10.1111/j.1471-8286.2004.00587.x

Rubini A, Paolocci F, Riccioni C, Vendramin GG, Arcioni S (2005) Genetic and phylogeographic structures of the symbiotic fungus *Tuber magnatum*. Appl Environ Microbiol 71(11):6584–6589. doi:10.1128/AEM.71.11.6584-6589.2005

Sisti D, Giomaro G, Zambonelli A, Rossi I, Ceccaroli P, Citterio B, Stocchi V, Benedetti PA (1998) In vitro mycorrhizal synthesis of micropropagated *Tilia platyphyllos* Scop. plantlets with Tuber borchii Vittad. mycelium in pure culture. Acta Hortic 457:379–387

Swofford DL (2000) PAUP*: phylogenetic analysis using parsimony (*and other methods). Version 4.0b10. Sinauer Associates, Sunderland

Taylor JW, Jacobson DJ, Kroken S, Kasuga T, Geiser DM, Hibbett DS, Fisher MC (2000) Phylogenetic species recognition and species concept in fungi. Fungal Genet Biol 31:21–32. doi:10.1006/fgbi.2000.1228

Taylor JW, Turner E, Townsend JP, Dettman JR, Jacobsom D (2006) Eukaryotic microbes, species recognition and the geographic limits of species: examples from the kingdom Fungi. Phil Trans R Soc B 361:1947–1963. doi:10.1098/rstb.2006.1923

Thompson JD, Higgins DG, Gibson TJ (2004) Clustal W: improving the sensitivity of progressive multiple alignment through sequence weighting, position-specific gap penalties and weight matrix choice. Nucleic Acid Res 22:4673–4680

Vittadini C (1831) Monographia tuberacearum. Felicis Rusconi, Milano

Walton WH (1948) Feret's statistical diameter as a measure of particle size. Nature 162:329–330. doi:10.1038/162329b0

Wang Y, Tan ZM, Zhang DC, Murat C, Jeandroz S, Le Tacon F (2006) Phylogenetic relationship between *Tuber pseudoexcavatum*, a Chinese truffle, and other Tuber species based on parsimony and distance analysis of four different gene sequences. FEMS Microbiol Lett 259:269–281. doi:10.1111/j.1574-6968.2006.00283.x

Wedén C, Danell E, Camacho FJ, Backlund A (2004) The population of the hypogeous fungus *Tuber aestivum* syn. *T. uncinatum* on the island of Gotland. Mycorrhiza 14:19–23. doi:10.1007/s00572-003-0271-4

Wedén C, Danell E, Tibell L (2005) Species recognition in the truffle genus Tuber—the synonyms *Tuber aestivum* and *Tuber uncinatum*. Environ Microbiol 7:1535–1546. doi:10.1111/j.1462-2920.2005.00837.x

Zambonelli A, Iotti M, Rossi I, Hall I (2000a) Interaction between *Tuber borchii* and other ectomycorrhizal fungi in a field plantation. Mycol Res 104(6):698–702. doi:10.1017/S0953756299001811

Zambonelli A, Rivetti C, Percudani R, Ottonello S (2000b) TuberKey: a delta-based tool for the description and interactive identification of truffles. Mycotaxon 74:57–76

Zambonelli A, Iotti M, Giomaro G, Hall IR, Stocchi V (2002) *T. borchii* cultivation: an interesting perspective. Edible mycorrhizal mushrooms and their cultivation. In: Hall I, Wang Y, Danell E, Zambonelli A (eds), Edible mycorrhizal mushrooms. Proceedings of 2nd international workshop on edible ectomycorrhizal mushrooms, New Zealand Institute for Crop and Food Research Limited, CD room. 3–6 July 2001, Christchurch, New Zealand